Factors Governing Light Attenuation in Upper Segments of the James and York Estuaries and Their Influence on Primary Producers

Rachel Henderson[1] · Paul A. Bukaveckas[1]

Abstract

Upper estuarine segments are characterized by mixing of diverse source waters with a variety of constituents that may influence water clarity (e.g., algae, inorganic particulates, dissolved color). We measured turbidity, total suspended solids (TSS), chlorophyll-a (CHLa), dissolved organic carbon (DOC), and chromophoric dissolved organic matter (CDOM) in upper segments of the James and York Estuaries to better understand their role in light attenuation. Turbidity and TSS were found to be the best predictors of inter-site and intra-site variations in light attenuation. CHLa was not found to be a strong predictor of light attenuation, indicating that suspended particulate matter was largely non-algal. CDOM played a greater role in light attenuation in the Pamunkey and Mattaponi sub-estuaries, which derive a greater proportion of their inflow from lowland (Coastal Plain) sources where extensive wetlands and floodplain forest likely serve as a source of CDOM. Although dissolved and particulate components of light attenuation were derived from external (watershed) sources, variation in external inputs (river discharge) was not a strong predictor of estuarine light attenuation. Analysis of long-term (25-year) data indicate trends of decreasing turbidity and increasing water clarity at some sites, coinciding with decreases in river sediment inputs. In the James Estuary, underwater light conditions remain below targets for successful SAV colonization and favor phytoplankton-dominated primary production. Management actions that reduce sediment loads are likely to be the most effective means for improving water clarity in upper estuarine segments.

Keywords Water clarity · Suspended particulate matter · Algal blooms · CDOM · Chesapeake Bay

Introduction

The depth to which sunlight penetrates the water column is an important attribute of aquatic ecosystems. Light penetration dictates the depth to which benthic algae and plants can colonize available habitat, and determines the light conditions experienced by phytoplankton circulating within the water column. Loss of water clarity constrains the depth range over which photosynthesis can occur, potentially altering the balance between photosynthesis and respiration (net ecosystem metabolism), and in turn, nutrient cycling and food web dynamics (Davies-Colley et al. 2014; Abdelrhman

✉ Paul A. Bukaveckas
pabukaveckas@vcu.edu

1   Center for Environmental Studies, Virginia Commonwealth University, 1000 West Cary Street, Richmond, VA 23284, USA

2017; Kim et al. 2020). Water clarity is especially important to shallow water bodies, including coastal lagoons and estuaries, as it is linked to the maintenance of two alternative stable states in which primary production is dominated by either macrophytes or phytoplankton (Bouska et al. 2020; Jones 2020; Yuan 2021). Shallow estuaries such as Chesapeake Bay historically supported extensive and diverse communities of submerged aquatic vegetation (SAV), which serve critical functions by absorbing excess nutrients, preventing sediment re-suspension and shoreline erosion, and providing habitat for commercial and recreational fisheries (Dennison et al. 1993). Since 1960, reductions in water clarity have caused SAV acreage to decrease throughout the Bay and its tributaries (Kemp et al. 2005; Baldizar and Rybicki 2006). Coinciding with this decline has been an increase in the occurrence of algal blooms, some of which are comprised of harmful algae (Morse et al. 2011; Egerton et al. 2014; Bukaveckas et al. 2018). Multiple agencies are working to develop and implement management strategies aimed at improving water clarity, restoring SAV, and mitigating

algal blooms. The success of these efforts depends in part on an understanding of the factors which contribute to light attenuation in various segments of the Bay and their influence on primary producers.

The diffuse attenuation coefficient (K_d) for photosynthetically active radiation (PAR) is a widely used measure of water clarity. Irradiance decreases exponentially with depth due to scattering of photons by suspended particulate matter and absorption of photons by water and its dissolved constituents (Kirk 2011; Gallegos 1994). Chromophoric dissolved organic matter (CDOM) is the fraction of DOC that contributes to light absorption. CDOM originates from decay of terrestrial and wetland plant material. Its importance to light attenuation in estuarine waters is determined by freshwater inputs, particularly from wetland sources. CDOM is not commonly measured in monitoring programs, and therefore, DOC is often used as a surrogate, though the proportional contribution of CDOM to DOC is variable (Zhao and Song 2018). Suspended particulate matter (SPM) causes scattering of photons, thereby increasing their path length and reducing their downward flux. SPM is comprised of non-living particles (e.g., clay, silt, and sand) as well as living cells (e.g., phytoplankton and bacteria). Light attenuation is affected by the abundance of particulates as well as their size and composition (Davies-Colley and Smith 2001; Davies-Colley et al. 2014). In general, finer materials have a greater negative impact on water clarity per unit mass. Two metrics commonly used to quantify SPM are total suspended solids (TSS), a gravimetric property (mass of SPM per volume), and turbidity, an optical property, which measures light scattering relative to standards. Chlorophyll-a (CHLa) is also commonly used to assess phytoplankton contributions to light attenuation. Statistical models relating light attenuation to DOC or CDOM, SPM, and CHLa are used to assess their relative importance across sites and over time (Gallegos and Moore 2000; Baldizar and Rybicki 2006; Chen and Doering 2016).

Quantifying the importance of various light attenuating factors is challenging due to their variable contributions under changing conditions. This is especially true in estuarine environments where the confluence of river water and sea water results in a diverse collection of optically active constituents from both terrestrial and aquatic sources. For example, CDOM concentrations vary along the length of the estuary, typically with higher concentrations near freshwater or wetland sources and lower concentrations seaward (Rochelle-Newall and Fisher 2002). Salinity has been used in some studies as a proxy for CDOM due to the negative relationship (e.g., Xu et al. 2005). Contributions from SPM also vary longitudinally, particularly where tidal forces lead to the formation of an estuarine turbidity maximum (McSweeney et al. 2017). Previous studies of Chesapeake Bay and Narragansett Bay found that TSS was a key factor affecting light attenuation (Gallegos 2001; Gallegos et al. 2005; Abdelrhman 2017) and Secchi depth (Testa et al. 2019). In a Florida estuary, CDOM and turbidity accounted for the greatest amount of variation in light attenuation, while CHLa was less important (Chen and Doering 2016). Our knowledge of inter-estuarine differences in the factors regulating water clarity is largely based on studies conducted in the lower, saline portions of the estuary. Less is known regarding the factors regulating water clarity in the upper estuary. Owing to their proximity to riverine inputs, upper estuarine segments receive episodic inputs of SPM during storm events (Bukaveckas et al. 2020). The upper estuary can also be a region of high phytoplankton production due to favorable nutrient and water residence time conditions (Wood and Bukaveckas 2014; Qin and Shen 2017). In this setting, the contributions of SPM to light attenuation may vary in response to storm events and algal blooms. Local tributaries may be an important source of CDOM, particularly where extensive wetland and floodplain area occur.

In this study, we measured light attenuation and associated variables (TSS, turbidity, DOC, CDOM, and CHLa) in upper segments of the James and York estuaries over a 3-year span (2017–2019). To characterize long-term trends, we analyzed similar data collected by the Chesapeake Bay Program over a 25-year span (1994–2019). Our main objective was to assess contributions from dissolved organic matter and suspended particulate matter to light attenuation. We tested univariate, linear models as well as multivariate, non-linear models (GAMs) to assess their utility in explaining variation in light attenuation. Lastly, we utilized our previously published data on phytoplankton abundance (CHLa) and production (GPP) in the James Estuary to test for relationships with water clarity. The overall goal was to improve understanding of factors regulating light attenuation in the upper estuary and how variation in light conditions affects primary producers.

Methods

Study Sites

This study focuses on the two southern tributaries of Chesapeake Bay (James and York Estuaries) and two sub-estuaries of the York (Pamunkey and Mattaponi). A prior paper documented inter-system differences in the influence of storm events on water quality and ecosystem metabolism in these estuaries (Bukaveckas et al. 2020). The proximity of the estuaries allowed us to conduct frequent sampling (1–2-week intervals) and to encompass a range of salinity conditions from tidal freshwater in the James, to oligohaline in the Pamunkey and Mattaponi, and mesohaline in the York (Fig. 1). We expected that algal
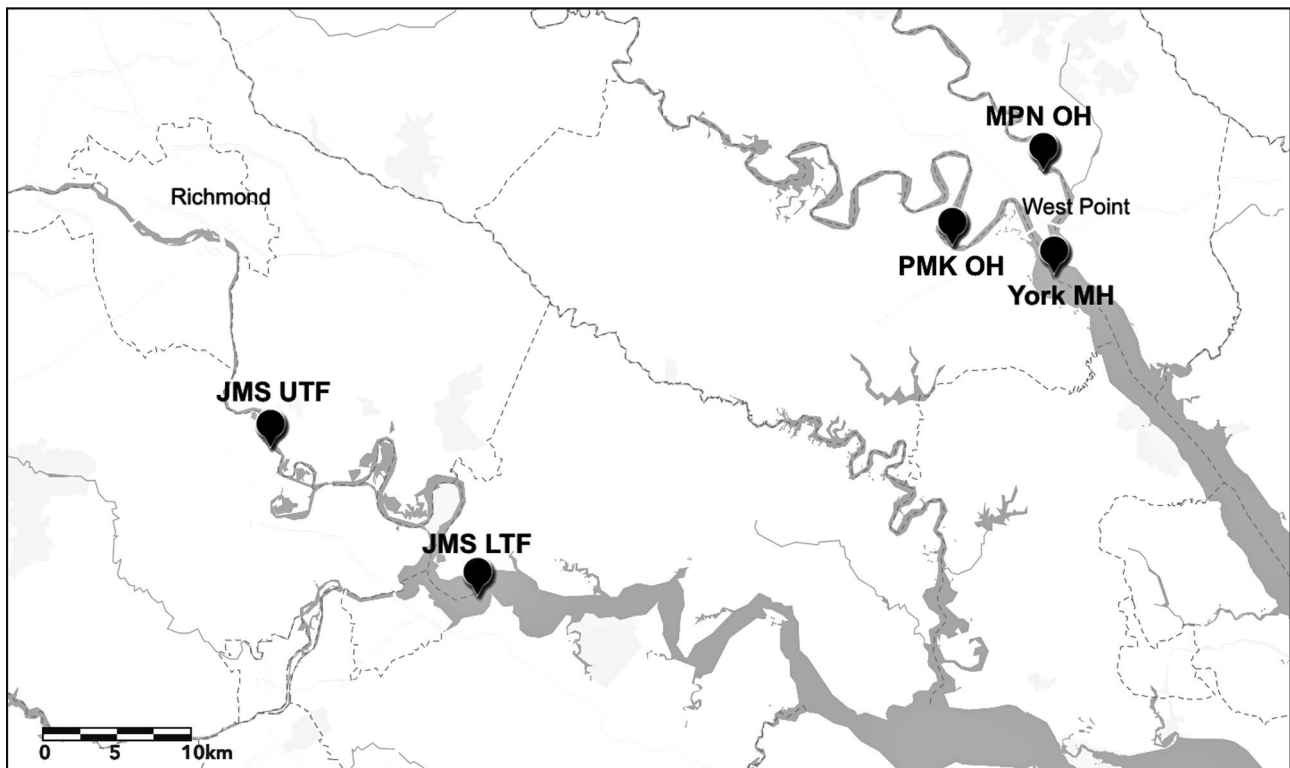
Fig. 1 Map of site locations in the James upper (JMS UTF) and lower (JMS LTF) tidal fresh segments, Mattaponi (MPN OH) and Pamunkey (PMK OH) oligohaline segments, and the York mesohaline (YRK MH) segment

contributions to light attenuation would be more important in the James based on our prior work documenting the occurrence of algal blooms in the tidal fresh segment (Bukaveckas et al. 2011, 2018; Tassone and Bukaveckas 2019). By contrast, the Pamunkey and Mattaponi are dominated by submerged and emergent vegetation with lower CHLa and GPP (Bukaveckas et al. 2020). We also anticipated that CDOM would be more important in the sub-estuaries of the York due to extensive wetlands and floodplains along the Mattaponi and Pamunkey (Hupp et al. 2009; Noe and Hupp 2009; Lake et al. 2013).

Sample Collection

Light attenuation and associated variables were measured at five sites including the upper and lower tidal fresh segments of the James (JMS UTF, LTF), oligohaline segments of the Mattaponi (MPN OH) and Pamunkey (PMK OH), and the mesohaline segment of the York (YRK MH). Sites were sampled by boat in the main channel. Data were collected on ~ 65 sampling dates from June 2017 through October 2019 (weekly in 2017 and bi-weekly in 2018 and 2019). During each sampling, water quality parameters (e.g., temperature and specific conductivity) were measured in the field using a YSI Pro DSS sonde. Irradiance (PAR) was measured

with a LI-COR model LI-1400 data logger equipped with underwater and surface quantum sensors (LI-192SA and LI-190SA, respectively). Underwater irradiance measurements consisted of vertical profiles at 0.5-m intervals with two or more replicate profiles obtained at each sampling. Light attenuation coefficients (K_d; m^{-1}) were derived from a linear regression of log-transformed down-welling irradiance versus depth (Kirk 2011). Water samples were obtained near the surface (< 1 m) and analyzed for TSS, turbidity, CHLa, and DOC. CDOM was measured for 1 year (beginning October 2018) at all sites except JMS UTF.

Sample Analysis

Water samples were analyzed by the VCU Environmental Analysis Lab, a state-accredited water quality testing facility. Turbidity was measured with a HACH model 2100 Turbidimeter. CHLa samples were filtered thru Whatman GF/A glass filters (0.5-µm nominal pore size), extracted for 18 h in buffered acetone and analyzed on a Turner Design TD-700 Fluorometer. TSS was determined gravimetrically using pre-weighed, pre-combusted filters (0.5 µm). DOC was measured by persulphate digestion followed by infrared detection using a Schimadzu TOC analyzer. CDOM samples were filtered (0.5 µm) and the filtrate analyzed at a wavelength

of 440 nm using a Schimadzu UV-1800 (5-cm pathlength) dual-beam spectrophotometer.

Other Data Sources

River discharge measured at USGS Fall Line stations was used to assess the influence of freshwater inputs on light attenuation and associated variables. Daily mean discharge was obtained from USGS stations on the James (at Richmond; #02037500), Appomattox (at Matoaca; #02041650), Mattaponi (near Beulahville; # 01674500), and Pamunkey Rivers (near Hanover; #01673000). Discharge for the JMS LTF site was calculated by combining daily values from the Richmond and Appomattox stations. Daily discharges for the York MH site were calculated by combining discharge values from the Mattaponi and Pamunkey stations. The 7-day mean discharge preceding each sampling event was used in the data analysis.

We supplemented data collected for this study with long-term data (1994–2019) from the Chesapeake Bay Program (obtained from CBP DataHub). Light attenuation data were available for two sites (TF5.5 and RET4.3) in the same locations as our study sites (JMS LTF and York MH, respectively). We also selected a station in the tidal fresh segment of the Pamunkey (TF4.2), which was in proximity to our PMK OH site. At each station, underwater light intensity was measured at depth intervals of either 0.25 or 0.5 m. Each station was visited on average 8 times a year at somewhat irregular intervals. Ancillary data for these sites included turbidity, TSS, CHLa, and DOC.

For the James, we assessed inter-annual variability in light availability for primary producers (see below), using incident PAR and turbidity data collected at the research pier of the VCU Rice Rivers Center, which is located ~2 km from the JMS LTF site (Bukaveckas et al. 2020). Turbidity data were collected at 15-min intervals using a YSI EXO2 water quality sonde and converted to daily average values. Sondes were calibrated every 2–3 weeks as per manufacturer's recommendations. Incident PAR data were collected at 15-min intervals using a LI-COR surface quantum sensor (LI-190SA) and converted to total daily values.

Data Analysis

Statistical analyses were performed to assess inter-site differences and to relate variation in light attenuation to variables potentially affecting water clarity. One-way ANOVAs were used to test for significant differences in light attenuation and ancillary variables among sites. To identify variables influencing light attenuation, we tested both univariate, linear models and multivariate, non-linear models. The former have the advantage that they can be parameterized from a

single measured variable (e.g., turbidity) and provide easily interpreted measures of effect size (e.g. the rate of change in light attenuation per unit of turbidity). Linear regressions were used to examine relationships between light attenuation and each of the predictor variables (turbidity, TSS, CHLa, DOC, CDOM, and discharge) and among the independent variables (e.g., turbidity vs TSS, CDOM vs DOC). For the multivariate, non-linear analysis, we used generalized additive models (GAMs). GAMs were used to model the effects of suspended solids (TSS or turbidity), algae (CHLa), and dissolved organic matter (CDOM or DOC) on light attenuation. GAMs are non-parametric, which makes them well-suited for non-normal data, and are capable of capturing non-linear relationships (Morton and Henderson 2008; Murphy et al. 2019; Yang and Moyer 2020). For modeling light attenuation, they have the advantage of depicting the response of K_d to each predictor variable, conditioned on all other variables. Long-term data from the Chesapeake Bay Program were also analyzed using GAMs to test for seasonal patterns and long-term trends. Predictor variables for modeling light attenuation were day of year (to describe seasonal patterns) and decimal date (to assess long term-trends). Similar models were tested to assess seasonal patterns and long-term trends in turbidity, TSS, CHLa, and DOC. Regressions and ANOVAs were performed using the "base" R package; GAMs were performed using the "mgcv" package in RStudio. The package default thin plate regression spline was used to depict inter-annual variability; a cyclic cubic regression spline was used to depict seasonal effects. All GAM results were scaled to center on the mean to assess the effect of each predictor variable.

For the James, we analyzed underwater light conditions and tested for relationships with CHLa and GPP. Underwater light conditions were characterized based on the average irradiance within the mixed layer, which in this case was equivalent to the average depth of the water column as neither temperature nor salinity gradients were present. The daily total irradiance averaged over the water column (I_{wc}; E m^{-2} day^{-1}) was derived using the equation from Gosselain et al. (1994):

$$Iwc = Is/(Kd \times Zmean).$$

where I_s is daily incident PAR (E m^{-2} day^{-1}), K_d (m^{-1}) is the light attenuation coefficient, and Z_{mean} is the average depth of the James lower tidal fresh segment (2.5 m). This analysis required daily estimates of K_d, which we derived from daily average values of turbidity obtained at the Rice Pier. The relationship between Pier turbidity and measured K_d at the nearby main channel station (JMS75) was modeled using a GAM, which also incorporated day of year as an explanatory variable (model $R^2 = 0.50$, $p < 0.001$). Model-derived daily K_d values were used along with measured

incident PAR to calculate daily underwater PAR (I_{wc}). We derived daily underwater PAR for April–October of each year (2017–2019) and determined the number of days within each year characterized by favorable light conditions. We considered favorable light conditions to be days when I_{wc} was greater than 5 E m^{-2} day^{-1} based on previous studies showing that riverine phytoplankton are predominantly light, not nutrient limited, when daily irradiance falls below this value (Koch et al. 2004). As prior work has documented the importance of water residence time in affecting algal bloom development in the James, we also considered the potential for interactive effects by determining how the occurrence of favorable light conditions varied in relation to discharge. We characterized dates when the preceding 7-day mean discharge was less than 100 m^3 s^{-1} (equivalent to ~30-day freshwater replacement time; FRT) as indicative of favorable water residence time conditions. Lastly, we used GAMs to depict the conditional response of CHLa to FRT and K_d, and to model monthly average daily GPP as a function of monthly average incident PAR (I_s), FRT and K_d. GPP data for this analysis were taken from Tassone and Bukaveckas (2019) and were derived from diel oxygen data collected at the Rice Pier.

Results

Estuarine Hydrology

Typical low discharge conditions during the outset of the study in summer-fall 2017 extended into winter 2017–2018 (Fig. 2). The persistence of baseflow conditions resulted in progressively increasing freshwater replacement times, which reached 150 days (Pamunkey), 100 days (Mattaponi), and 80 days (James). Thereafter, followed a prolonged period of above average discharge, which extended from winter-spring 2018 to include summer and fall of 2018 and winter-spring 2019. Due to unusually high precipitation during this period, discharge during the 2019 water year (October 2018 to September 2019) ranked in the top 10%-tile of long-term annual average values for all three rivers. Over this 15-month span (March 2018 to June 2019), freshwater replacement time was consistently low (e.g., James mean = 12 days) and well below typical summer values (James = 50–60 days). The concluding portion of the study (July to October 2019) marked a return to typical low summer discharge and longer freshwater replacement time. Overall, the 3-year study encompassed a wide range of discharge and FRT conditions, but could be characterized as having unusually high river inputs due to above average rainfall in 2018.
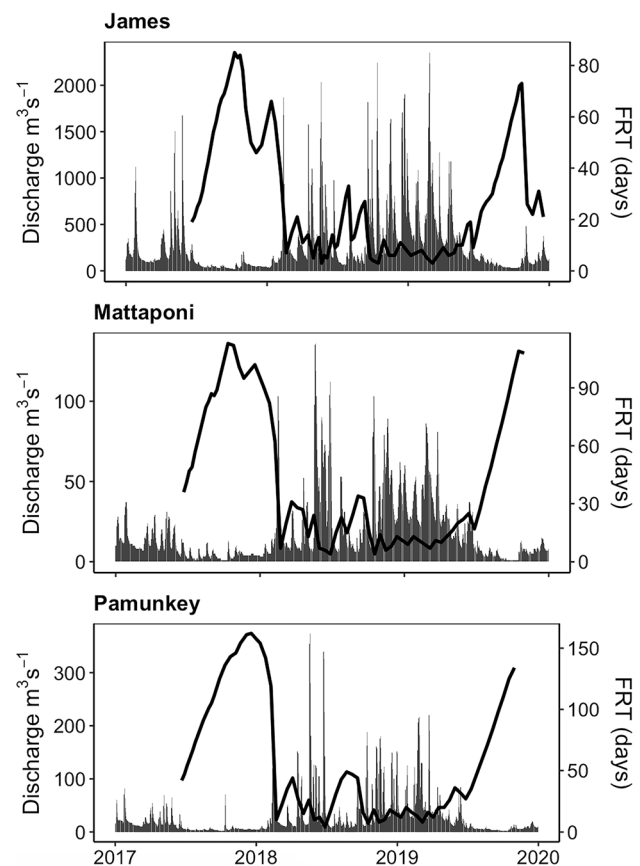
Fig. 2 Daily average instantaneous discharge (bars) and estuarine freshwater replacement time (FRT, lines) of the James, Pamunkey, and Mattaponi during the period of study (2017–2019)

Factors Influencing Water Clarity

The estuaries exhibited significant differences in light attenuation and associated water clarity variables (Fig. 3). The JMS upper tidal fresh site had the greatest water clarity, while the Mattaponi and Pamunkey sites had the lowest water clarity. Average light attenuation ranged from 1.85 ± 0.15 m^{-1} (JMS UTF) to 3.23 ± 0.11 m^{-1} (PMK OH), corresponding to photic depths (1% light penetration) of 2.5 m (JMS UTF) and 1.4 m (PMK OH). Inter-site differences in light attenuation tracked patterns in turbidity and TSS, with higher values observed among the Mattaponi, Pamunkey, and York sites relative to the James sites ($p < 0.001$). The James sites also exhibited significantly lower CDOM ($p = 0.025$) and DOC ($p < 0.001$) relative to the Mattaponi, Pamunkey and York sites. Inter-site differences in CHLa did not follow light attenuation or other variables, as highest CHLa was observed at the JMS lower tidal fresh and York sites, with lower and similar levels among the other 3 sites.

Univariate, linear regressions were used to test for relationships between light attenuation with turbidity, TSS, CDOM, and CHLa. Light attenuation was positively
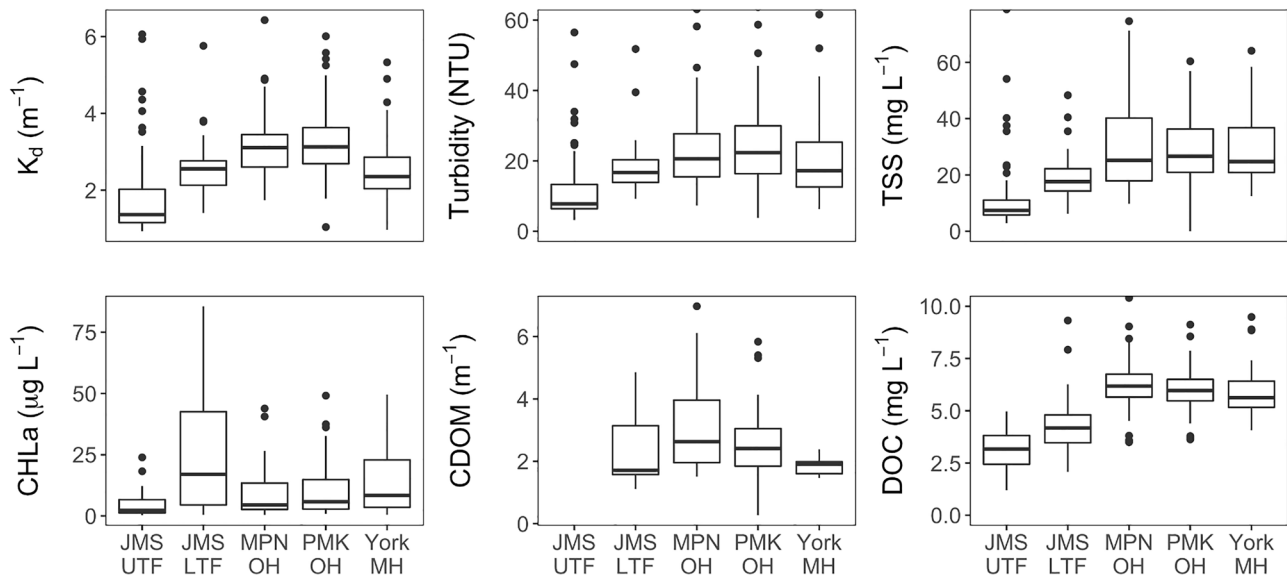
Fig. 3 Inter-site differences in light attenuation (K_d), turbidity, TSS, CHLa, CDOM, and DOC among stations in the James upper (JMS UTF) and lower (JMS LTF) tidal 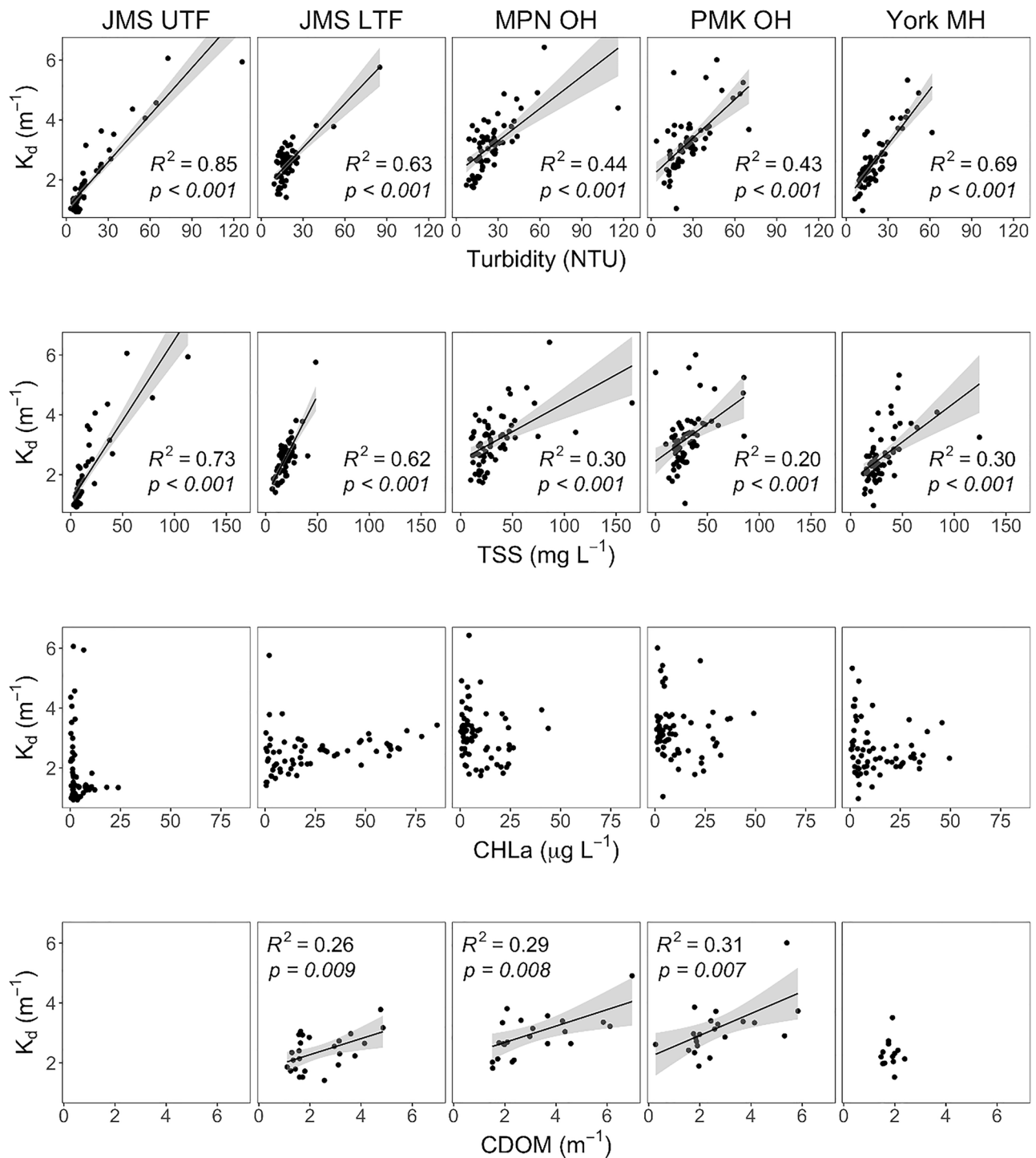fresh segments, Mattaponi (MPN OH) and Pamunkey (PMK OH) oligohaline segments, and the York mesohaline (York MH) segment (some outliers not visible)

correlated with turbidity and TSS at each of the five sites, though model parameters (slope and correlation) differed among sites (Fig. 4). The James sites generally exhibited stronger correlations between light attenuation and turbidity or TSS relative to the Mattaponi, Pamunkey, and York sites. Across sites, models based on turbidity accounted for a greater proportion of variation in light attenuation ($R^2 = 0.43$ to 0.85) than models based on TSS ($R^2 = 0.20$ to 0.73). Regression slopes indicate that the rate of change in K_d as a function of turbidity was higher among the JMS UTF (0.052 ± 0.003 m^{-1} NTU^{-1}) and JMS LTF (0.050 ± 0.005 m^{-1} NTU^{-1}) sites relative to the Mattaponi (0.036 ± 0.005 m^{-1} NTU^{-1}) and Pamunkey (0.043 ± 0.006 m^{-1} NTU^{-1}) sites. TSS models yielded similar results with larger slopes for the JMS UTF and LTF sites (0.054 ± 0.004 and 0.068 ± 0.007 m^{-1} mg^{-1} L^{-1}, respectively) compared to the Mattaponi, Pamunkey and York sites (range $= 0.019$ to 0.026 m^{-1} mg^{-1} L^{-1}). Turbidity and TSS were themselves significantly correlated at each of the sites ($p < 0.001$) though the strength of the relationship varied among sites ($R^2 = 0.28$ to 0.85; data not shown). Regression slopes indicate that the amount of turbidity per unit of TSS was twofold higher at the JMS UTF and LTF sites (1.03 ± 0.06 and 0.99 ± 0.13 NTU mg^{-1} L^{-1}, respectively) compared to the Mattaponi, Pamunkey, and York sites (range $= 0.38$ to 0.54 NTU mg^{-1} L^{-1}). Light attenuation was significantly positively correlated with CDOM at 3 of the 4 sites (excluding York; no data for JMS UTF). At the JMS LTF site, CDOM accounted for a smaller proportion of the variation in light attenuation ($R^2 = 0.26$) relative to turbidity

($R^2 = 0.63$) and TSS ($R^2 = 0.62$), whereas at the Mattaponi and Pamunkey sites, the proportion of variation explained by CDOM was comparable to the SPM variables. CHLa was not a significant predictor of light attenuation in univariate models for any of the 5 sites. DOC was not significantly correlated with light attenuation or CDOM at any of the sites.

Light attenuation and related variables were affected by variations in river discharge at some, but not all sites (Fig. 5). Discharge accounted for a small but significant proportion of the variation in K_d at two sites (JMS UTF and York MH). At these sites, as well as the JMS LTF site, there was a significant positive effect of discharge on turbidity ($R^2 = 0.14$ to 0.35; $p < 0.01$). Increases in discharge were also associated with higher CDOM as indicated by significant positive relationships at 3 of the 4 sites (excluding York; $R^2 > 0.50$, $p < 0.001$). We also tested the utility of salinity (specific conductance) as a predictor of variations in CDOM. We found that CDOM declined with increasing conductivity as indicated by significant negative relationships at 3 of the 4 sites (excluding York). The proportion of variation in CDOM accounted for by conductivity was consistently lower than models based on discharge ($R^2 = 0.18$ to 0.52; data not shown).

Generalized additive models were used to depict the conditional response of light attenuation to each of the predictor variables (turbidity, CHLa and DOC; Fig. 6). The GAMs accounted for over 70% of the variation in light attenuation at each site, except for the Pamunkey ($R^2 = 0.44$). Turbidity exhibited the greatest influence on light attenuation with K_d increasing from ~2 to >5 m^{-1}
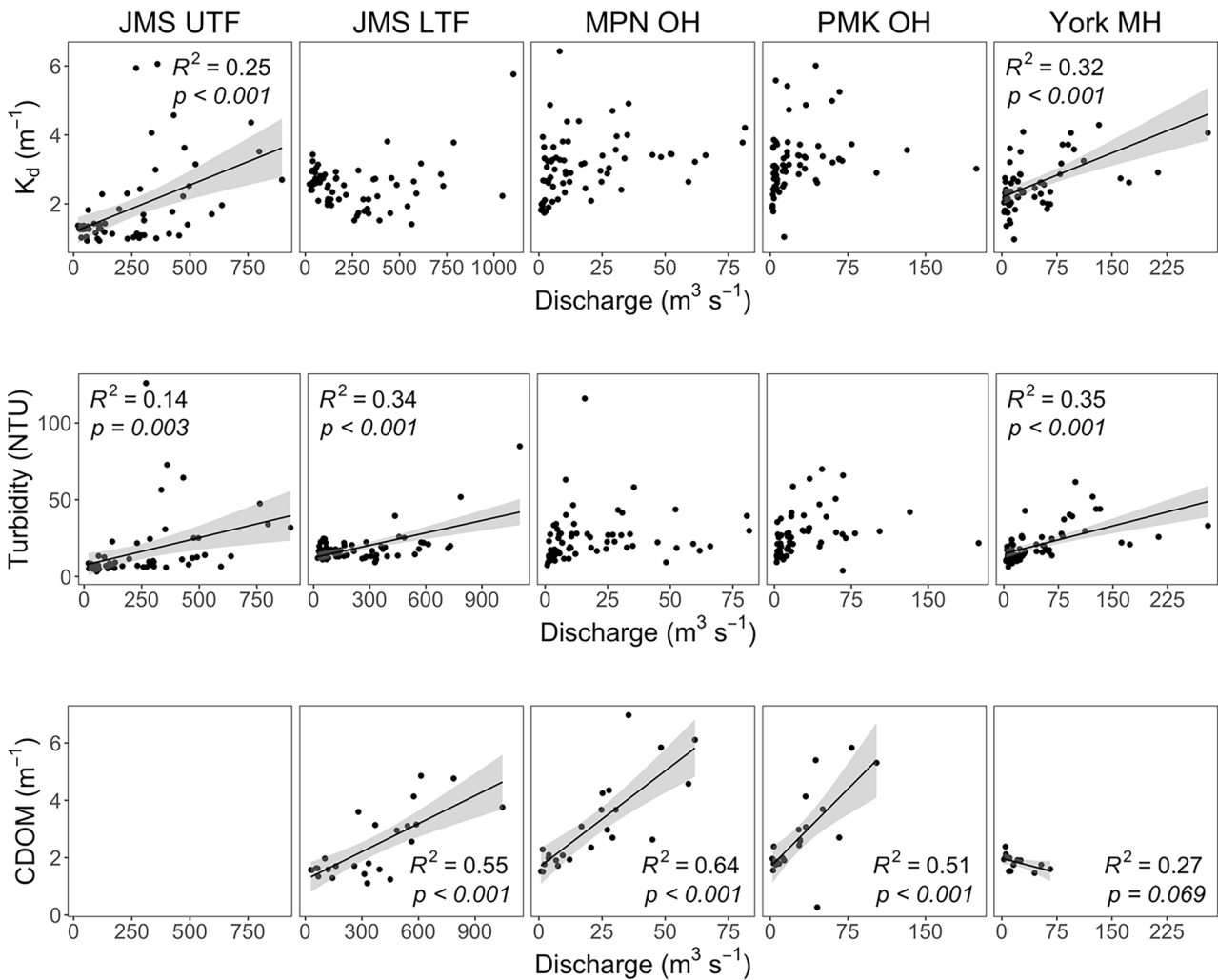
Fig. 4 Relationships between light attenuation (K_d) and turbidity, TSS, chlorophyll-a (CHLa), and CDOM for the James River upper (JMS UTF) and lower (JMS LTF) tidal fresh segments, Mattaponi (MPN OH) and Pamunkey (PMK OH) oligohaline segments, and the York mesohaline (York MH) segment. Regression lines are for models with statistically significant results ($p < 0.05$)

over a range of turbidity from 10 to 60–70 NTU. By contrast, DOC exhibited weak, and in most cases not significant effects on light attenuation. DOC was used in this analysis rather than CDOM due to the greater time span

of data, and the availability of data for all five sites. Substituting CDOM for DOC in the GAM analysis yielded a significant effect at only one site (JMS LTF, $p = 0.002$). There was a significant positive effect of CHLa on light

Fig. 5 River discharge as a predictor of estuarine light attenuation, turbidity, and CDOM in the James River upper (JMS UTF) and lower (JMS LTF) tidal fresh segments, Mattaponi (MPN OH) and Pamunkey (PMK OH) oligohaline segments, and the York mesohaline (York MH) segment (no CDOM for JMS UTF). Models with statistically significant results ($p < 0.05$) display regression lines

attenuation at JMS LTF ($p = 0.009$) and York ($p < 0.001$), which were the sites exhibiting highest CHLa (up to 80 and 50 µg L^{-1}, respectively). The range of response in light attenuation to increasing CHLa (from ~ 2.2 to 2.6 m^{-1}) was small in comparison to the effects of turbidity. Overall, the multivariate, non-linear models accounted for a greater proportion of the variation in light attenuation than the best univariate, linear models based on turbidity alone. The change in light attenuation was nearly linear over the full range of turbidities observed at the James (UTF and LTF) and Mattaponi sites, whereas at the Pamunkey and York sites, light attenuation plateaued in the higher range of turbidities (> 40 NTU).

Implications for Primary Producers

The availability of long-term monitoring data for the James tidal fresh segment allowed us to assess the influence of variable water clarity on GPP and CHLa. The occurrence of light and discharge conditions favorable for algal bloom development varied considerably between years. In 2017, favorable conditions were observed on 34% of days during the growing season, whereas in the year with high discharge (2018), the frequency of occurrence was only 9% (Fig. 7). Differences between the two years were largely due to the direct effects of discharge as the proportion of dates indicating favorable water residence time conditions

Fig. 6 Results of GAM analysis depicting the effects of turbidity, DOC, and chlorophyll-a (CHLa) on light attenuation in the James (JMS), Mattaponi (MPN), Pamunkey (PMK), and York estuaries. R^2 values are the total variation explained by the three predictor variables
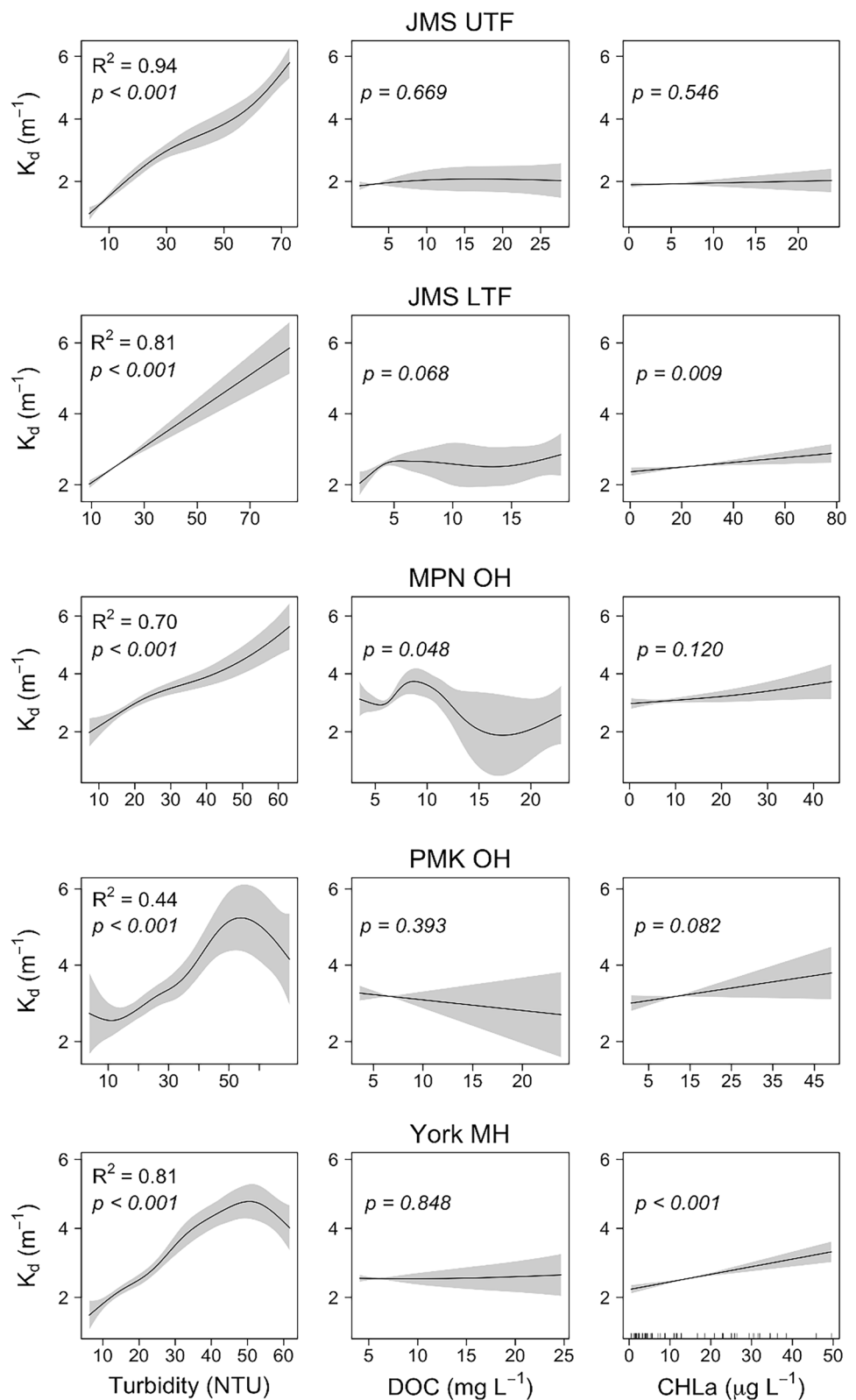
(discharge < 100 m³ s⁻¹) differed by fourfold (58 and 13% in 2017 and 2018, respectively). By comparison, the proportion of dates with favorable light conditions was more similar

between years (63 and 55%, respectively). The GAM analysis revealed that both freshwater replacement time and light attenuation were significant predictors of CHLa ($p < 0.001$

Fig. 7 Water clarity conditions in the lower tidal fresh segment of the James and linkages to phytoplankton abundance and production. Upper panels: frequency of occurrence of favorable light (I_{wc} > 5 E m^{-2} day^{-1}) and discharge (< 100 m^3 s^{-1}) conditions during April–October of 2017 and 2018. Middle panels: GAM results predicting CHLa based on freshwater replacement time (FRT) and light attenuation (K_d). Lower panels: GAM results predicting monthly average GPP based on incident solar radiation (PAR), FRT and K_d
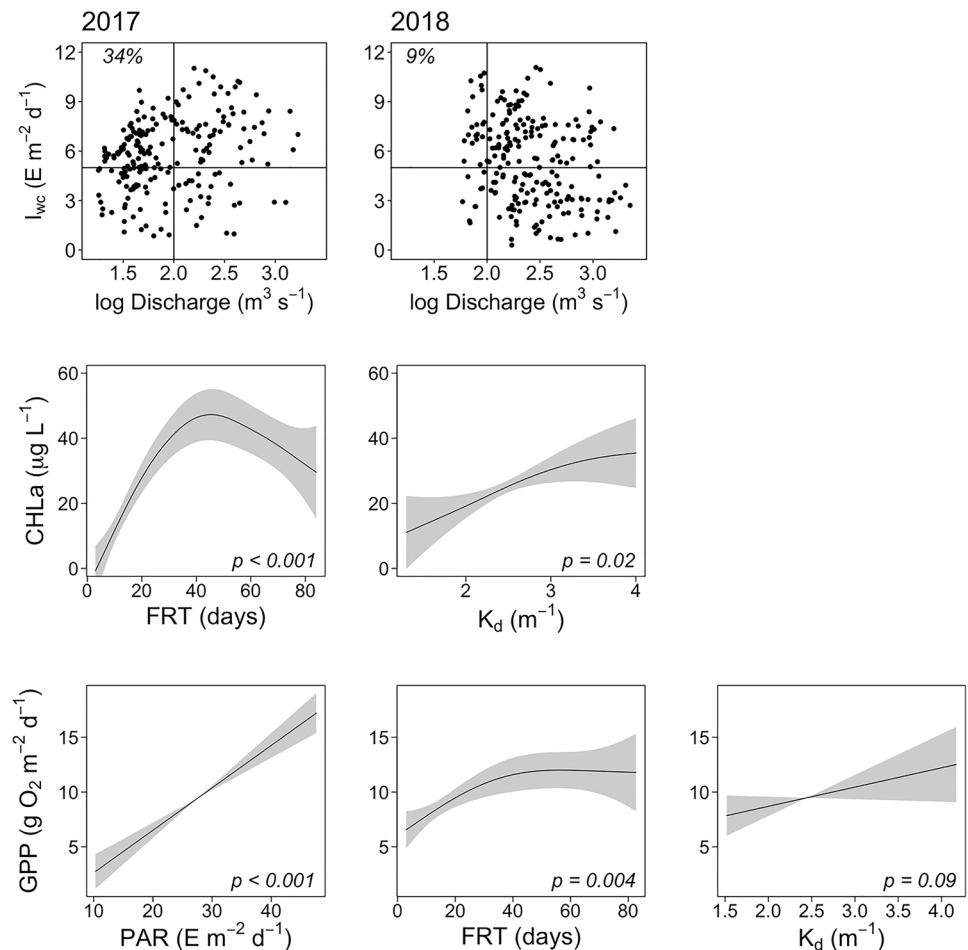
and $p = 0.02$, respectively). CHLa showed a near linear increase up to a freshwater replacement time of ~ 40 days, and declined somewhat thereafter. CHLa was also positively related to light attenuation though the range of response (~ 15 µg L^{-1}) was small in comparison to the effects of FRT (~ 45 µg L^{-1}). The overall model accounted for 58% of the variation in CHLa (RMSE = 14.4). Monthly averages of daily GPP were found to be significantly related to incident PAR ($p < 0.001$) and FRT ($p = 0.004$) and marginally related to light attenuation ($p = 0.09$). The largest range of response for GPP was observed in relation to incident PAR (from 3 to 18 g O$_2$ m^{-2} day^{-1}). GPP exhibited a smaller range of response in relation to FRT (from 7 to 12 g O$_2$ m^{-2} day^{-1}) and light attenuation.

Long-term Trends

GAM analysis of Chesapeake Bay Program data revealed long-term trends of decreasing light attenuation at the York MH ($p = 0.007$) and James LTF ($p = 0.054$) sites (Fig. 8; Table 1). At both sites, light attenuation declined from ~ 3.6 m^{-1} to 2.8 m^{-1} over a 25-year span, corresponding

to an increase in photic depth from 1.3 to 1.6 m. Declines in light attenuation were accompanied by significant decreasing trends in turbidity from ~ 28 to ~ 15 NTU ($p = 0.028$ and $p < 0.001$ for JMS and York, respectively). The Pamunkey site exhibited a marginally significant increasing trend in light attenuation ($p = 0.074$) but no significant trend in turbidity. There were no significant long-term trends in DOC or CHLa among the three sites. The York and Pamunkey sites exhibited similar seasonal patterns in light attenuation with summer minimum values of ~ 2.5 m^{-1} following spring maxima of 3.5–4.0 m^{-1} (data not shown). Seasonal patterns in light attenuation tracked patterns in turbidity. No consistent seasonal patterns in light attenuation or turbidity were observed in the James.

Discussion

Our findings indicate that suspended particulate matter is the primary agent affecting light attenuation among upper segments of the James and York Estuaries. In univariate models, SPM, whether measured as TSS or turbidity, was

Fig. 8 Results from GAM analysis depicting long-term trends in light attenuation, turbidity, and DOC among sites in the James lower tidal fresh, Pamunkey tidal fresh, and York mesohaline (data from Chesapeake Bay Program)
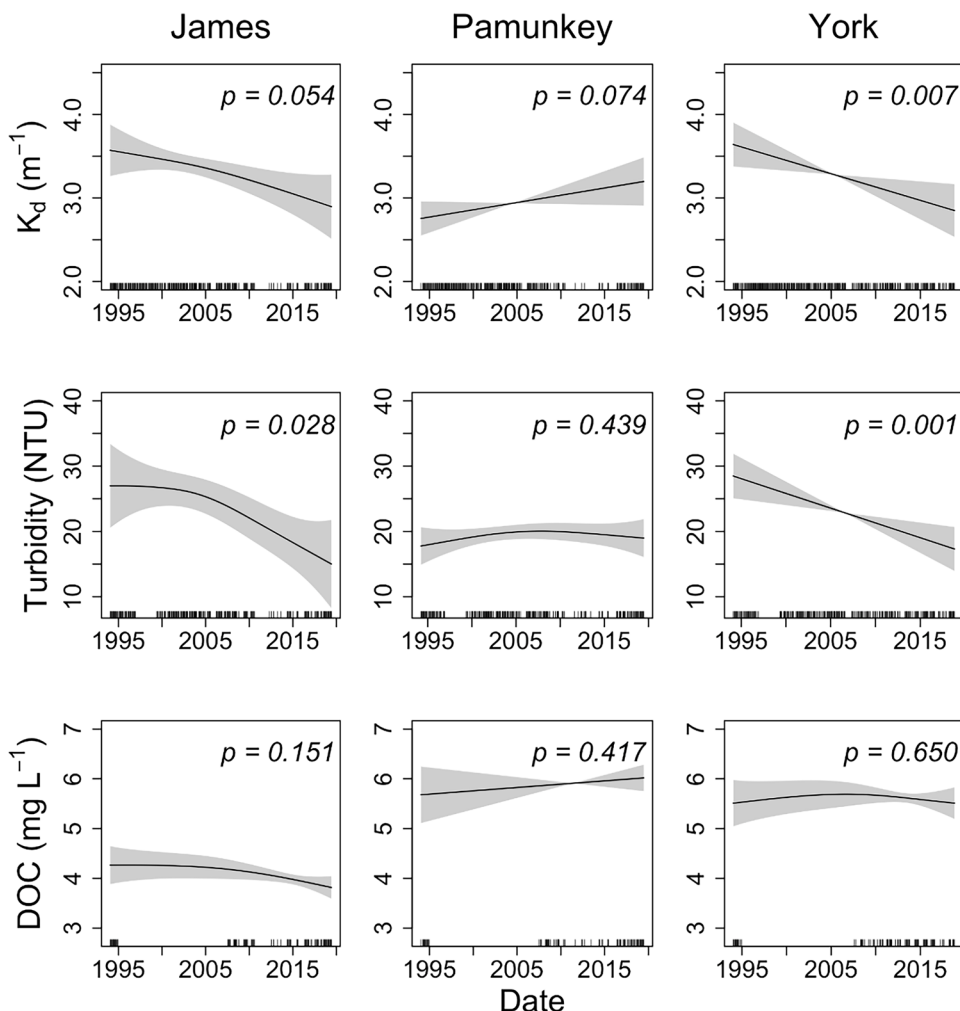
the best predictor of light attenuation at all sites. In multivariate models (GAMs), SPM was associated with a larger range of response in light attenuation than was observed for other variables. We observed mostly linear responses in light attenuation to increasing turbidity and TSS over

the full range of measured values. The Pamunkey and York sites were an exception in that we observed a saturating response in light attenuation at the high end of the range (turbidity > 40 NTU). At high turbidities, the photic zone is compressed and the standard method of quantifying

Table 1 Results of GAM analysis depicting seasonal (day of year; DoY) and inter-annual (date) effects on light attenuation (K_d), turbidity, chlorophyll-a (CHLa), and DOC based on data collected at Chesapeake Bay Program monitoring stations (1994–2019)

Model	Site	Segment	Adj. R^2	RMSE	s (DoY)	p (DoY)	s (Date)	p (Date)
Kd	James	LTF	0.06	1.28	1.30	0.054	4.53	0.046
	Pamunkey	TF	0.11	1.02	1.00	0.074	3.67	< 0.001
	York	MH	0.17	1.24	1.00	0.007	2.62	< 0.001
Turbidity	James	LTF	0.07	19.6	4.03	0.10	1.74	0.028
	Pamunkey	TF	0.26	8.6	3.44	< 0.001	1.66	0.44
	York	MH	0.27	13.2	3.72	< 0.001	1.00	< 0.001
CHLa	James	LTF	0.45	14.2	3.43	< 0.001	8.51	0.009
	Pamunkey	TF	0.19	4.6	2.00	< 0.001	6.18	0.008
	York	MH	0.14	14.0	4.00	0.002	7.55	0.026
DOC	James	LTF	0.38	0.68	5.20	< 0.001	1.47	0.15
	Pamunkey	TF	0.21	1.07	3.00	< 0.001	1.00	0.42
	York	MH	0.08	0.76	1.85	0.026	1.50	0.65

underwater irradiance at fixed depth intervals yields fewer observations in the measureable range. We cannot discount the possibility that the apparent plateau in light attenuation is an artifact of having fewer measurements, though we did not observe this effect at the James and Mattaponi sites at similar turbidity levels. Profiles obtained during high turbidity conditions yielded correlation coefficients comparable to those for profiles collected during low turbidity conditions ($R^2 > 0.90$). Using turbidity alone (univariate linear models), we were able to predict light attenuation with an RMSE of 0.40 to 0.65 across sites. This range of errors corresponds to 16 to 23% of the average light attenuation. By comparison, the non-linear multivariate models had lower RMSs (0.25 to 0.44) corresponding 11 to 14% of mean values. Our findings suggest that light attenuation at these sites can be modeled reasonably accurately based on turbidity alone, but that inclusion of DOC and CHLa, and the use of non-linear models, provided stronger predictive power.

In these upper estuarine segments, externally-derived (non-algal) particulates were the main source of suspended particulate matter. CHLa was generally a weak predictor of inter- and intra- site variation in light attenuation, despite high CHLa levels observed at two of the sites (JMS LTF, York MH). Prior work in the James, based in part on stable C isotopes, showed that algae comprise up to 60% of the organic component of SPM during the summer peak (Wood et al. 2016), but the overall organic content of SPM was low ($17 \pm 1\%$), indicating that the bulk of this material is inorganic. The large catchment of the James River encompasses upland areas in the Piedmont and Appalachian Mountain regions where erosion and sediment yield is high (Gellis et al. 2009). By comparison, the Mattaponi and Pamunkey are mostly situated in the lowland Coastal Plain where erosive forces are weaker. Differences in sediment loads among these basins may explain why stronger correlations between SPM and light attenuation were observed in the James relative to the Pamunkey and Mattaponi. We also detected differences in effect size in that light attenuation increased more rapidly per unit of TSS or turbidity in the James relative to the Pamunkey and Mattaponi. Though we lack data on particle size, these findings suggest that the delivery of finer materials from the James watershed may exert stronger negative effects on water clarity. Overall, our hypothesis that phytoplankton should play a greater role in influencing water clarity in the James was not supported due to the over-riding effects of external inputs of inorganic particulate matter.

Although our findings indicate that SPM is the primary component of light attenuation, dissolved substances were important to inter-estuarine differences. Our ability to model their effects was constrained by limited CDOM data (1 year) and by the fact that DOC was not a useful surrogate for CDOM at these sites. Positive correlations between CDOM and DOC have been reported in both fresh and marine waters (Bukaveckas & Robbins-Forbes 2000; Ferrari 2000; Rochelle-Newall and Fisher 2002; Stedmon et al. 2003). The lack of correlation at our sites may be due to mixing of diverse source waters (Fall Line inputs, local runoff, and tidal inputs from the lower estuary), which differ in the chromophoric component of DOC. Despite limited data, the results show elevated CDOM in the Pamunkey and Mattaponi relative to the James and York. In the Pamunkey and Mattaponi, the proportion of variation in light attenuation accounted for by CDOM was comparable to that of SPM, whereas in the James, neither CDOM nor DOC were strong predictors of site-specific variation in light attenuation. Another means of assessing the potential importance of CDOM is by comparing intercepts for the relationship between light attenuation and turbidity. The intercept represents the potential contribution of water and dissolved substances to light attenuation in the absence of turbidity (i.e., predicted K_d at turbidity $= 0$). Larger intercepts were derived for the Mattaponi (2.22 m^{-1}) and Pamunkey (2.08 m^{-1}) relative to the James (1.62 m^{-1}) and York (1.33 m^{-1}). The intercepts were strongly correlated with average CDOM ($R^2 = 0.94$, $p = 0.029$). These findings are consistent with our hypothesis that extensive wetland and floodplain areas adjacent to the Pamunkey and Mattaponi serve as important source areas for CDOM. These estuaries derive a larger proportion of their hydrologic inputs from local runoff relative to Fall Line inputs. Local (ungauged) inputs were estimated based on the proportion of contributing area below the Fall Line (James $= 10\%$, Mattaponi $= 51\%$, Pamunkey $= 36\%$). The Pamunkey and Mattaponi receive a greater proportion of inputs from within the Coastal Plain, which is characterized by sandy soils with limited capacity to retain DOC. By comparison, the James Estuary is more constricted, with minimal floodplain and wetland areas, and receives a greater proportion of hydrologic inputs from sources above the Fall Line (i.e., outside the Coastal Plain). These findings suggest that differences in the geomorphic settings of the estuaries may account for the greater importance of CDOM to light attenuation in the Pamunkey and Mattaponi.

Light attenuation was principally controlled by external inputs of SPM and CDOM, rather than internally derived sources of particulate matter via algal production. Despite this, we did not find that light conditions in these estuaries were highly sensitive to external forcing events, despite unusually high river discharge during the study period. Discharge accounted for a small proportion of the variation in light attenuation in the James upper tidal fresh segment, and in the York, but was not a significant predictor of K_d at the Pamunkey, Mattaponi or James LTF sites. Prior work has shown that during high discharge, sediment inputs at the Fall Line are rapidly attenuated down the estuary, in part due to the delivery of heavier materials during events (Bukaveckas et al. 2019; 2020). At locations more distant form the Fall

Line (e.g., James LTF, PMK and MPN OH), there is little change in light attenuation in response to elevated Fall Line discharge. For these analyses, we used the 7-day average discharge preceding each sampling event. Data on transit times from the Fall Line to each sampling location might allow us to better align variation in discharge with estuarine responses, though analyses using shorter and longer average discharge values did not improve these relationships. Our findings suggest that internal processes (tidal forces) were more important to maintaining suspended loads than the external drivers (storm events) regulating their delivery to the estuary. Strong tidal forces act to maintain a relatively constant suspended sediment load irrespective of changes in sediment delivery at the Fall Line. Interestingly, discharge was a stronger predictor of CDOM than for TSS or turbidity. Increases in estuarine CDOM with elevated discharge may be due to displacement of DOC-rich water from surface and sub-surface storage zones following rain events (Zarnetske et al. 2018). In these low salinity segments, we did not find that conductivity was a strong predictor of CDOM, as has been observed in studies spanning a broader range of salinity conditions (Xu et al. 2005).

We have previously shown that elevated discharge affects the metabolic balance of the James and Pamunkey estuaries due to larger declines in GPP relative to respiration (Bukaveckas et al. 2020). We attributed the suppression of GPP during high discharge to flushing effects (advective loss) on phytoplankton. In this paper, we show that reduced GPP following storm events cannot be attributed to diminished water clarity as light attenuation in the James LTF was not appreciably affected by discharge. More broadly, our data suggest that freshwater replacement time has a larger effect on phytoplankton biomass and production in the James than water clarity, given the current range of water clarity conditions. Near-linear increases in both GPP and CHLa were observed up to a water residence time of ~40 days, beyond which there was little change. These findings suggest that with prolonged low discharge conditions, other factors (e.g., nutrient limitation, grazing) may exert greater control over production and biomass accrual as also indicated by recent modeling studies (Qin and Shen 2021). Seasonal factors such as incident solar radiation act to broadly constrain GPP, but there was little additional explanatory power gained from inclusion of water clarity in models predicting GPP. Current water clarity conditions likely act to maintain a stable state of phytoplankton-dominated production in the James due to constraints on SAV colonization imposed by the shallow photic depth. Despite the limited photic depth (~1.5 m), the broad and relatively shallow channel (mean depth = 2.5 m) provides favorable light conditions for phytoplankton in comparison to the deeper, more constricted upper tidal fresh segment. A partial release from light limitation, along with longer water residence time, results in high

GPP and recurring algal blooms (CHLa up to 100 µg L^{-1}) in this segment of the James.

Water clarity conditions are improving at some sites, but are insufficient to facilitate a transition from phytoplankton to SAV dominance. Analysis of the Chesapeake Bay Program data showed that light attenuation at the James (LTF) and York sites has decreased by ~20% over a 25-year span. The improvement in water clarity corresponds to a decrease in turbidity, but no change in CHLa. A recent analysis of flow-normalized trends has shown that suspended sediment loads reaching the Fall Line of the James have declined by 20% from 1985 to 2019 (Moyer and Blomquist 2020). These trends, along with our data showing weak relationships between CHLa and light attenuation, suggest that declining inputs of inorganic particulate matter are the likely cause for improvements in water clarity, rather than declines in algal abundance. The large (> 50%) reduction in nutrient loads to the James Estuary following upgrades to wastewater treatment plants (Bukaveckas & Isenberg 2013) have not appreciably reduced phytoplankton abundance. This is in marked contrast to recent changes in nearby Gunston Cove (Potomac Estuary) where reductions in point source inputs led to reductions in CHLa (from > 80 to 20 µg L^{-1}), decreased light attenuation (from 3.7 to 2.0 m^{-1}), and recovery of SAV over the span from 1991 to 2017 (Jones 2020). Monitoring of SAV by the Virginia Institute of Marine Science shows that coverage in the James lower tidal fresh segment has increased from < 40 ha prior to 2005 to greater than 200 ha in recent years. Despite their expansion, SAV coverage remains very limited (~1% of total area) likely because the James is too deep given current water clarity conditions. The CBP considers an irradiance of 13% (relative to sub-surface) at 1 m to be the minimum light requirement for SAV growth in tidal fresh and oligohaline segments (Batiuk et al. 2000). The larger decrease in light attenuation at Gunston Cove (by 1.7 m^{-1}) relative to the James (by 0.8 m^{-1}) resulted in an increase in light at 1 m from 2 to 14%. Over a similar time span, light reaching 1 m in James increased from 3 to 6% of sub-surface. If the current trend continues, we predict that the James tidal fresh segment may attain the minimum light requirement by 2044.

Conclusions

Overall, our findings indicate that suspended particulate matter was the primary factor affecting inter-site and intra-site variation in light attenuation among upper segments of the James and York Estuaries. SPM metrics, whether measured as turbidity or TSS, yielded stronger correlations and larger effect sizes for the James sites, which may reflect the greater contribution of fine particulate matter originating from mountainous areas in the upper watershed. CDOM

played a greater role in light attenuation among segments receiving a greater proportion of runoff from lowland (Coastal Plain) sources (Pamunkey and Mattaponi Estuaries). The algal fraction of SPM was not an important component of light attenuation owing to the high proportion of inorganic suspended particulates. These findings suggest that management actions focusing on reducing sediment loads (e.g., stream bank and bed stabilization) may have a greater benefit for improving water clarity in the upper estuary than nutrient reductions to limit phytoplankton biomass. Long-term monitoring data from the Chesapeake Bay Program indicate that increases in water clarity and decreases in turbidity have been accompanied by a modest expansion of SAV coverage at some sites. If trends observed over the past 25 years continue over the next 25 years, light penetration may be sufficient to favor a shift from a phytoplankton- to SAV-dominated state, as has been observed in other systems. Characterizing the underwater light climate in turbulent, turbid systems remains a challenge, though recent advances in sensor technology and modeling efforts have shed light on the interactions between flow, depth, and water clarity (Gardner et al. 2019; Wang et al. 2021). We hope findings presented here provide a better understanding of factors regulating light attenuation in the upper estuary and aid in management decisions aimed at restoring estuarine water clarity.

References

Abdelrhman, M.A. 2017. Quantifying contributions to light attenuation in estuaries and coastal embayments: Application to Narragansett Bay, Rhode Island. *Estuaries and Coasts* 40: 994–1012.

Baldizar, J.M., and N.B. Rybicki. 2006. Primary factors affecting water clarity at shallow water sites throughout the Chesapeake and Maryland coastal bays. Proceedings of the Eighth Federal Interagency Sedimentation Conference 1027–1034.

Batiuk, R.A., P. Bergstrom, M. Kemp, E. Koch, L. Murray, J. Court Stevenson, R. Bartleson, et al. 2000. Chesapeake Bay submerged aquatic vegetation water quality and habitat-based requirements and restoration targets: A second technical thesis. Annapolis, MD, USA: Chesapeake Bay Program; EPA.

Bouska, K.L., J. N. Houser, N.R. De Jager, D.C. Drake, S.F. Collins, D.K. Gibson-Reinemer, and M. A. Thomsen. 2020. Conceptualizing alternate regimes in a large floodplain-river ecosystem: Water clarity, invasive fish and floodplain vegetation. *Journal of Environmental Management* 264: 110516.

Bukaveckas, P.A., and M. Robbins-Forbes. 2000. The role of dissolved organic carbon in the attenuation of photosynthetically active and ultraviolet radiation in Adirondack lakes. *Freshwater Biology* 43: 339–354.

Bukaveckas, P.A., L.E. Barry, M.J. Beckwith, V. David, and B. Lederer. 2011. Factors determining the location of chlorophyll maximum and the fate of algal production within the tidal freshwater James River. *Estuaries and Coasts* 34 (3): 569–582.

Bukaveckas, P.A., and W.N. Isenberg. 2013. Loading, transformation, and retention of nitrogen and phosphorus in the tidal freshwater James River (Virginia). *Estuaries and Coasts* 36 (6): 1219–1236.

Bukaveckas, P.A., R.B. Franklin, S. Tassone, B. Trache, and T.A. Egerton. 2018. Cyanobacteria and cyanotoxins at the river-estuarine transition. *Harmful Algae* 76: 11–21.

Bukaveckas, P.A., M. Katarzyte, A. Schlegel, R. Spuriene, T. Egerton, and D. Vaiciute. 2019. Composition and settling properties of suspended particulate matter in estuaries of the Chesapeake Bay and Baltic Sea regions. *Journal of Soil and Sediments* 19: 2580–2593.

Bukaveckas, P.A., S. Tassone, W.M. Lee, and R.B. Franklin. 2020. The influence of storm events on metabolism and water quality of riverine and estuarine segments of the James, Mattaponi and Pamunkey Rivers. *Estuaries and Coasts* 43: 1585–1602.

Chen, Z.C., and P.H. Doering. 2016. Variation of light attenuation and the relative contribution of water quality constituents in the Caloosahatchee River Estuary. *Florida Scientist* 79 (2–3): 93–108.

Davies-Colley, R.J., and D.G. Smith. 2001. Turbidity, suspended sediment, and water clarity: A review. *Journal of the American Water Resources Association* 37 (5): 1085–1101.

Davies-Colley, R.J., D.J. Ballant, S.H. Elliot, A. Swales, A.O. Hughes, and M.P. Gall. 2014. Light attenuation—A more effective basis for the management of fine suspended sediment than mass concentration? *Water Science & Technology* 69: 1867–1874.

Dennison, W.C., R.J. Orth, J.C. Stevenson, V. Carter, S. Kollar, P.W. Bergstrom, and R.A. Batiuk. 1993. Assessing water quality with submersed aquatic vegetation. *BioScience* 43 (2): 86–94.

Egerton, T.A., R.E. Morse, H.G. Marshall, and M.R. Mulholland. 2014. Emergence of algal blooms: The effects of short-term variability in water quality on phytoplankton abundance, diversity, and community composition in a tidal estuary. *Microorganisms* 2: 33–57.

Ferrari, G.M. 2000. The relationship between chromophoric dissolved organic matter and dissolved organic carbon in the European Atlantic coastal area and in the West Mediterranean Sea (Gulf of Lions). *Marine Chemistry* 70 (4): 339–357.

Gallegos, C.L. 1994. Refining habitat requirements of submersed aquatic vegetation: Role of optical models. *Estuaries* 17 (1): 198–219.

Gallegos, C.L., and K.A. Moore. 2000. Factors contributing to water-column light attenuation. In Chesapeake Bay submerged aquatic vegetation water quality and habitat-based requirements and restoration targets: a second technical synthesis, by R.A. Batiuk, 35–54. Annapolis, MD: EPA Chesapeake Bay Program.

Gallegos, C.L. 2001. Calculating optical water quality targets to restore and project submersed aquatic vegetation: Overcoming problems in partitioning the diffuse attenuation coefficient for photosynthetically active radiation. *Estuaries* 24 (3): 381–397.

Gallegos, C.L., T.E. Jordan, A.H. Hines, and D.E. Weller. 2005. Temporal variability of optical properties in a shallow, eutrophic estuary: Seasonal and interannual variability. *Estuarine, Coastal, and Shelf Science* 64 (2–3): 156–170.

Gardner, J.R., S.H. Ensign, J.N. Houser, and M.W. Doyle. 2019. Light exposure along particle flowpaths in large rivers. *Limnology and Oceanography*. https://doi.org/10.1002/lno.11256.

Gellis, A.C., and others, 2009. Sources, transport, and storage of sediment in the Chesapeake Bay Watershed. U.S. Geological Survey Scientific Investigations Report 2008–5186.

Gosselain, V., J.P. Descy, and E. Everbecq. 1994. The phytoplankton community of the River Meuse, Belgium: Seasonal dynamics (year 1992) and the possible incidence of zooplankton grazing. *Hydrobiologia* 289 (1): 179–191.

Hupp, C.R., A.R. Pierce, and G.B. Noe. 2009. Floodplain geomorphic processes and environmental impacts of human alteration along Coastal Plain rivers, USA. *Wetlands* 29: 413–429.

Jones, R.C. 2020. Recovery of a tidal freshwater embayment from eutrophication: A multi-decadal study. *Estuaries and Coasts* 43: 1318–1334.

Kemp, W.M., W.R. Boynton, J.E. Adolf, D.F. Boesch, W.C. Boicourt, G. Brush, J.C. Cornwell, T.R. Fisher, P.M. Glibert, J.D. Hagy, L.W. Harding, E.D. Houde, D.G. Kimmel, W.D. Miller, R.I.E. Newell, M.R. Roman, E.M. Smith, and J.C. Stevenson. 2005. Eutrophication of Chesapeake Bay: Historical trends and ecological interactions. *Marine Ecology Progress Series* 303: 1–29.

Kim, G.E., P. St-Laurent, M.A.M. Friedrichs, and A. Mannino. 2020. Impacts of water clarity variability on temperature and biogeochemistry in the Chesapeake Bay. *Estuaries and Coasts* 43: 1973–1991.

Kirk, J.T.O. 2011. *Light and Photosynthesis in aquatic ecosystems*, 3rd ed. New York, NY: Cambridge University Press.

Koch, R.W., D.L. Guelda, and P.A. Bukaveckas. 2004. Phytoplankton growth in the Ohio, Cumberland and Tennessee Rivers, USA: Inter-site differences in light and nutrient limitation. *Aquatic Ecology* 38: 17–26.

Lake, S.J., M.J. Brush, I.C. Anderson, and H.I. Kator. 2013. Internal versus external drivers of periodic hypoxia in a coastal plain tributary estuary: The York River, Virginia. *Marine Ecology Progress Series* 492: 21–39.

McSweeney, J.M., R.J. Chant, J.L. Wilkin, and C.K. Sommerfield. 2017. Suspended sediment impacts on light limited productivity in the Delaware Estuary. *Estuaries and Coasts* 40: 977–993.

Morse, R.E., J. Shen, J.L. Blanco-Garcia, W.S. Hunley, S. Fentress, M. Wiggins, and M.R. Mulholland. 2011. Environmental and physical controls on the formation and transport of blooms of the dinoflagellate Cochlodinium polykrikoides Margalef in the lower Chesapeake Bay and its tributaries. *Estuaries and Coasts* 34: 1006–1025.

Morton, R., and B.L. Henderson. 2008. Estimation of non-linear trends in water quality: An improved approach using generalized additive models. *Water Resources Research* 44: W07420.

Moyer, D.L. and J.D. Blomquist. 2020. Nitrogen, phosphorus, and suspended-sediment loads and trends measured at the Chesapeake Bay River Input Monitoring stations—Water years 1985–2019: U.S. Geological Survey data release, https://doi.org/10.5066/P9VG459V.

Murphy, R.R., E. Perry, J. Harcum, and J. Keisman. 2019. A generalized additive model approach to evaluating water quality: Chesapeake Bay case study. *Environmental Modelling and Software* 118: 1–13.

Noe, G.B., and C.R. Hupp. 2009. Retention of riverine sediment and nutrient loads by Coastal Plain floodplains. *Ecosystems* 12: 728–746.

Qin, Q., and J. Shen. 2017. The contribution of local and transport processes to phytoplankton biomass variability over different time scales in the Upper James River, Virginia. *Estuarine, Coastal and Shelf Science* 196: 123–133.

Qin, Q., and J. Shen. 2021. Typical relationships between phytoplankton biomass and transport time in river-dominated coastal aquatic systems. *Limnology and Oceanography*. https://doi.org/10.1002/lno.11874.

Rochelle-Newall, E.J., and T.R. Fisher. 2002. Chromophoric dissolved organic matter and dissolved organic carbon in Chesapeake Bay. *Marine Chemistry* 77 (1): 23–41.

Stedmon, C.A., S. Markager, and R. Bro. 2003. Tracing dissolved organic matter in aquatic environments using a new approach to fluorescence spectroscopy. *Marine Chemistry* 82: 239–254.

Tassone, S.J., and P.A. Bukaveckas. 2019. Seasonal, interannual, and longitudinal patterns in estuarine metabolism derived from diel oxygen data using multiple computational approaches. *Estuaries and Coasts* 42 (1): 1032–1051.

Testa, J.M., V. Lyubehich, and Q. Zhang. 2019. Patterns and trends in Secchi disk depth over three decades in the Chesapeake Bay estuarine complex. *Estuaries and Coasts* 42: 927–943.

Wang, Z., F. Chai, H. Xue, X. H. Wang, Y. J. Zhang, R. C. Dugdale, and F. B. Wilkerson. 2021. Light regulation of phytoplankton growth in San Francisco Bay studied using a 3D sediment transport model. *Frontiers in Marine Science* 8: 633707.

Wood, J.D., and P.A. Bukaveckas. 2014. Increasing severity of phytoplankton nutrient limitation following reductions in point source inputs to the tidal freshwater segment of the James River Estuary. *Estuaries and Coasts* 37: 1188–1201.

Wood, J.D., D. Elliot, G. Garman, D. Hopler, W.M. Lee, S. McIninch, A.J. Porter, and P.A. Bukaveckas. 2016. Autochthony, allochthony and the role of consumers in influencing the sensitivity of aquatic systems to nutrient enrichment. *Food Webs* 7: 1–12.

Xu, J., R.R. Hood, and S.Y. Chao. 2005. A simple empirical optical model for simulating light attenuation variability in a partially mixed estuary. *Estuaries and Coasts* 28 (4): 572–580.

Yang, G., and D.L. Moyer. (2020) Estimation of non-linear water quality trends in high-frequency monitoring data. *Science of the Total Environment* 715: 136686.

Yuan, L.L. 2021. Continental-scale effects of phytoplankton and non-phytoplankton turbidity on macrophyte occurrence in shallow lakes. *Aquatic Sciences* 83: 14.

Zarnetske, J.P., M. Bouda, B.W. Abbott, J. Saiers, and P.A. Raymond. 2018. Generality of hydrologic transport limitation of watershed organic carbon flux across ecoregions of the United States. *Geophysical Research Letters* 45: 11702–11711.

Zhao, Y., and K. Song. 2018. Relationships between DOC and CDOM based on the total carbon-specific fluorescence intensities for river waters across China. *Journal of Geophysical Research: Biogeosciences* 123: 2353–2361.